Supplementary Material

Methods

Patients

Patient 1 is a 19-year-old male whose medical history is notable for progressive development of neutropenia, and mild chronic thrombocytopenia. In addition, he suffered from aphthous ulcers since age 3 years complicated by secondary bacterial infections, periodontitis with multiple missing teeth, and recurrent pulmonary and soft tissue infections. During adolescence he developed severe warts on the hands and feet, that were unresponsive to multiple topical and systemic agents. On initial presentation to the NIH, the diagnosis of large granular lymphocytic leukemia was made first, and he was treated with weekly methotrexate with improvement in his neutropenia. Upon discontinuation of methotrexate, he was treated with low-dose daily G-CSF, with sustained increase in the absolute neutrophil count. Since initiation of G-CSF treatment in 2017, he has not had issues with aphthous ulcers and has had only two episodes of cellulitis. Family history is non-contributory.

Patient 2 is a 50-year-old male who was diagnosed with common variable immunodeficiency (CVID) at age 37 due to low IgG, high IgM, recurrent sinopulmonary infections, refractory multi-lineage cytopenias as well as hepato-splenomegaly and autoimmune thyroid disease. Infectious history prior to his diagnosis of CVID is unremarkable. His first episode of immune-mediated thrombocytopenia (ITP) occurred at five years of age followed by multiple episodes throughout his life. At age 40 years he developed autoimmune hemolytic anemia (AIHA) and neutropenia. Cytopenias became increasingly refractory to therapies including various combinations of high-dose immunoglobulin, high-dose steroids, rituximab, romiplostim, eltrombopag, fostamatinib, and cyclosporine. The neutropenia was non-responsive to G-CSF. Monthly immunoglobulin replacement therapy has helped reduce the frequency of sinopulmonary infections. Family history is not notable for any other male relatives with similar clinical findings.

Patient 3 was a 27-year-old male with a history of recurrent bacterial sinopulmonary and skin infections, warts, candida esophagitis and hypogammaglobulinemia since 2 years of age. Since early childhood, he suffered from multiple episodes of AIHA, ITP, and presumed autoimmune

neutropenia which responded to high-dose IVIG, rituximab, and G-CSF. He continued to require IVIG with cycles of yearly rituximab for the next ten years in the attempt to control his cytopenias. Subsequently, the patient was maintained on oral steroids and intermittent G-CSF with limited efficacy. Bone marrow biopsies consistently showed hypocellular marrow with normal trilineage hematopoiesis and, most recently, infiltrating TCR$\gamma\delta^+$ T cell clones that were also present in peripheral blood. As a teenager, mediastinal adenitis was noted on chest imaging, and in the setting of an indeterminate QuantiFERON Gold test, the patient was treated for tuberculosis with no improvement of the lymphadenopathy. Around the same time, the patient developed noncaseating granulomatous lesions of the skin on the lower legs, later found to also be present in the lungs, bone marrow, and liver; infectious work up was negative. Medical history is also notable for Blount's disease as a child requiring multiple surgeries and persistent tibia vara, autoimmune hypothyroidism, hypophosphatemia, intermittent bradycardia, autoimmune enteropathy, nodular regenerative hyperplasia of the liver, inflammatory synovitis of his joints, mild developmental delay, and subtle dysmorphic features of the face (malar hypoplasia and slightly cupped ears). At the age of 27 years, the patient developed multiple strokes at another institution, leading to death. Post-mortem examination was not performed.

Patient 4 was a 56-year-old adopted male referred for evaluation and treatment of progressive multifocal leukoencephalopathy (PML). No data are available on his past medical history in childhood. Hypogammaglobulinemia, recurrent autoimmune multi-lineage cytopenias, as well as bacterial and viral infections have been documented since young adulthood. Cytopenias were refractory to splenectomy, intermittent IVIG, high-dose corticosteroids, and rituximab (last dose 1 year prior to onset of PML). Infectious history is notable for severe VZV infection as a child followed by shingles at age 36, warts on the hands, bacterial meningitis secondary to mastoiditis at age 44, pneumococcal meningitis at age 50, septic arthritis, sepsis, and recurrent sinopulmonary infections. At age 55, he developed a diffuse granulomatous rash of the limbs and trunk that on biopsy was reported as neurocutaneous sarcoidosis.

PML onset started with change in vision, followed three months later by behavioral changes and expressive aphasia. The diagnosis of PML was ultimately made by typical MRI findings of multifocal T2 hyperintense lesions with no contrast enhancement. JC virus CSF viral copy number of 32,000/mL at the time of diagnosis that rapidly increased to 6,740,500/mL. At 56 years of life, the patient passed away from complications of PML.

Methods

Flow cytometry

Peripheral blood and bone marrow aspirate blood were processed using Ficoll (GE Healthcare, Malborough, MA) to obtain peripheral blood mononuclear cells (PBMCs) and buffy coats and to form a single cell suspension and then stained with the following monoclonal antibodies directed against cell surface antigens:

CD4-APCCy7, CD25-PECy7, CD8-PB, CD3-BV605 (all from BD Pharmingen, Franklin Lakes, NJ), CD127-PerCP Cy5.5, CXCR5-AF647, CCR6-PE, CD20-FITC, CD16- CD57-BV421, CD45 APCCy7, CD34 PE, CD10 PECy7 (all from BD Biosciences, San Jose, CA), CD3-APC, CD45RA-FITC, CD71-APC (all from eBioscience, San Diego, CA), CD3-BV605, CD98-FITC, CD8-PE-Dazzle, CD4-PE, Va-7.2-PE, CD161-BV510, CD95-BV605, PD1-BV510, CD244-PE, CXCR4-PECy5, CXCR4-APC, CD4-PE, CXCR3-BV42, CD20 FITC, IgM PB, CD38 BV510, CD138 PE/Dazzle, CD19 PerCpCy5.5 (all from Biolegend, San Diego, CA), CD3/CD56-FITC/PC5, CD14-FITC (all from Beckman Coulter, Brea, CA), GLUT1-AF700 (R&D Systems, Minneapolis, MN), CD22 APC (Miltenyi Biotec, Gaithersburg, MD), CD4-APC (BD Pharmingen), Fc blocker and live/dead dye. Upon washing, cells were analyzed by flow cytometry using LSR Fortessa Flow Cytometer (BD) using FACSDiva software (BD). Final analysis was done using FlowJo v.10.6 (TreeStar). CXCR4 staining was performed on whole blood.

Whole exome sequencing

Genomic DNA was extracted from peripheral blood samples, and subjected to massively parallel (NextGen) sequencing on an Illumina (San Diego, CA) sequencing system.

The exonic regions, flanking splice junctions and both 5' and 3' untranslated regions (UTR) were sequenced with 100bp or greater paired-end reads. Subsequently, the reads were aligned to the human genome build GRCh37/UCSC hg19 and analysis was performed using a custom-enhanced analysis tool (SEQR). The interpretation of the variants was performed according to the ACMG guidelines[1] and the nomenclature of the identified variants is consistent with the Human Genome Variation Society (HGVS) guidelines[2]. Confirmation of potentially relevant

findings was performed using capillary sequencing or other appropriate method. Minimum coverage was 95% > 20X for targeted genomic regions.

NK cells phenotyping and NK cells degranulation and IFNγ production.

Peripheral blood was collected in EDTA containing vacutainers. Red blood cells were lysed from 200 µl of EDTA-blood using RBC lysis buffer (eBioscience). Cells were washed with FACS buffer (PBS containing 2% FBS), then stained according to previously published methods.[3] The antibodies used to define NK cell phenotype were either commercially available or were generated in the laboratories of Alessandro Moretta and Silvia Parolini (Brescia, Italy).

To assess IFN-γ production, PBMCs were incubated overnight at 37°C with IL-12 (0.5 ng/mL) and IL-18 (0.1 ng/mL), and intracellular IFN-γ production was evaluated by flow-cytometry upon gating on $CD3^-$ $CD56^+$ cells.

To analyze NK cell degranulation, PBMCs were co-cultured with K562 target cells at an effector:target ratio of 1:3 in a final volume of 200 µl in round-bottomed 96-well plates at 37°C and 5% CO2 for 4 h in culture medium supplemented with anti-CD107a-PE monoclonal antibody (BD Biosciences Pharmingen, San Diego, CA, USA) with or without IL-2 (100 IU/mL). Cells were surface-stained with FITC-anti-CD3, PC5 anti-CD56, FITC anti-CD14 (Beckman Coulter), FITC anti-CD20, and APC/Cy7 anti-CD16 (BD Biosciences) monoclonal antibodies for 30 min at 4°C, then washed. The proportion of $CD3^-$ $CD14^-$ CD20- $CD56^+$ cells expressing CD107a (a marker of degranulation) was analyzed by flow cytometry.

Cell proliferation assay

PBMCs were isolated to form a single cell suspension and then stained with 1mM Cell Trace Violet (CTV) (Thermo Fisher, Carlsbad, CA) for 20 minutes at 37°C in phosphate-buffered saline. Cells where then washed, resuspended in RPMI containing 10% fetal bovine serum, plated in a 48-well plate at a concentration of 5×10^5 cells per well, and then cultured with either medium alone (no stimulation), 20 ng/mL PMA (Sigma Aldrich, St. Louis, MO) in combination with 500ng/mL ionomycin (Sigma Aldrich), or 100 ng/mL anti-CD3 (eBioscience) in combination with 100 ng/mL anti-CD28 (eBioscience) with or without 100 U/mL recombinant human IL-2 (NIH) for 4 days. The cells were then stained for flow cytometry as indicated previously, and proliferation was assessed by CTV dilution.

Cell cycle and apoptosis assay

PBMCs at a concentration of 5 x 10^5 cells per well were cultured with either medium alone (no stimulation), 20 ng/mL PMA (Sigma Aldrich) in combination with 500 ng/mL ionomycin (Sigma Aldrich), or 100 ng/mL anti-CD3 (eBioscience) in combination with 100 ng/mL anti-CD28 (eBioscience) for 72 hours and then stained.

For cell cycle analysis, EdU incorporation into patient T cells was evaluated using Click-iT™ EdU Alexa Fluor 647 - Flow Cytometry Assay Kit from Invitrogen following the manufacturer's instructions.

For apoptosis analysis, cells were stained with FITC-ANNEXIN V apoptosis detection kit (Biolegend) and DAPI (Fx cycle™ violet, Invitrogen) for 30 minutes and analyzed by flow cytometry.

Western blot

For protein analysis, PBMCs (1x10^6 cells) or CD3 enriched T cells (5x10^5 cells) (EasySep Human T cell enrichment kit (19051), Stemcell technologies) under resting condition or after stimulation for 20 minutes with CD3/CD28 (Dynabeads T cell activator, Invitrogen, Carlsbad, CA) were utilized to obtain protein lysate from patients and controls. Samples were resolved on SDS-PAGE according to standard protocols, transferred to nitrocellulose transfer membrane (Invitrogen), and immunoblotted with different antibodies. Immunoreactive proteins were detected with horseradish peroxidase–coupled secondary antibodies (GE Healthcare), followed by ECL (Thermo Scientific, Waltham, MA). For loading control, the membrane was costained or stripped then stained with a monoclonal antibody against Beta-actin (Cell Signaling Technology Boston, MA).

The antibodies used in the experiments were as follows: anti-SASH3 rabbit polyclonal (PA570305, Invitrogen), anti p-PLCγ1monoclonal (14008), anti PLCγ1 polyclonal (2822), anti p-AKT polyclonal (9271), anti AKT polyclonal (9272), anti p-ZAP70/Syk monoclonal (2717), anti ZAP70 monoclonal (3165), anti p-LAT polyclonal (3584), anti p-S6 polyclonal (2215), anti p-mTOR monoclonal (5536), anti p-4EBP monoclonal (2855), anti p-ERK monoclonal (4377), anti p-p65 monoclonal (3033), anti p-IκBα monoclonal (2859), anti Bcl2 monoclonal (15071), anti Bim monoclonal (2933) (all from Cell Signaling Technology).

High throughput sequencing (HTS) of TCRα rearrangements.

PBMCs were collected and enriched for CD3 (Pan T cell isolation kit, Miltenyi Biotec). The TCRα (*TRA*) rearranged genomic products were amplified by multiplex polymerase chain reaction (PCR) using DNA as the template (Adaptive Biotechnologies Seattle, WA). Adaptive Biotechnologies uses assay-based and computational techniques to minimize PCR amplification bias. The assay is quantitative, and the frequency of a given *TRA* sequence is representative of the frequency of that clonotype in the original sample. The PCR products were sequenced using the Illumina HiSeq platform. Custom algorithms were used to filter the raw sequences for errors and align the sequences to reference genome sequences. Subsequently, the data were analyzed using the ImmunoSeq set of online tools. Distribution of the frequency of individual clonotypes (including *TRAV* to *TRAJ* pairing) and use of individual *TRAV* genes were analyzed within unique sequences. Heat map representation of the frequencies of individual *TRAV* to *TRAJ* gene pairs was produced using R software version 3.6.3 (2020-02-29). TCR self-reactivity was evaluated by analyzing amino acid composition and hydrophobicity at positions 6 and 7 of the TRA CDR3 on unique and total reads, as previously described[4].

In vitro T cell differentiation of bone-marrow derived CD34$^+$ cells

CD34$^+$ CD3$^-$ cells were sort-purified from the bone marrow of patient P2 and from mobilized peripheral blood of a healthy control. *In vitro* T cell differentiation was performed as described[5], by combining CD34$^+$ CD3$^-$ cells with MS5-hDLL4 cells in artificial thymic organoids (ATO), which were cultured in complete RB27 medium supplemented with rhIL-7 (5 ng/mL), rhFlt3-L (5 ng/mL) and 30 μM l-ascorbic acid 2-phosphate sesquimagnesium salt hydrate. *In vitro* progression of T cell development was monitored by staining for T cell differentiation markers as previously described in referenced paper[5].

Generation and characterization of SASH3$^{-/-}$ Jurkat cells

To generate *SASH3$^{-/-}$* Jurkat clones, two pairs of DNA oligonucleotides were designed in order to generate guide RNAs binding target regions in exon1 and intron 1 of the *SASH3* gene, respectively. The sequence of the DNA oligonucleotides is as follows:

SASH3 exon 1 gRNA1: 5'-CACCGGAGGGCTTGCGGCGCAGCA

SASH3 exon 1 gRNA 1: 3'rC-AAACTGCTGCGCCGCAAGCCCTCC
SASH3 intron 1 gRNA 2: 5'-CACCGGTTGGCTCCATCTCGGGTA
SASH3 intron 1 gRNA 2: 3'rC-AAACTACCCGAGATGGAGCCAACC.
Each pair of DNA oligonucleotides was annealed and cloned into either the PX458 (Addgene, Cambridge, MA, USA) or the PX459 (Addgene) plasmid digested by *Bpi*I. Both plasmids were transfected into the Jurkat clone E6-1 using AMAXA™ P3 primary cell 4D-Nucleofector™ X kit S (Lonza, Köln, Germany) following the manufacturer's protocol. At 24h after transfection, GFP-positive cells were isolated and dispersed into single cells using limiting dilution. A few weeks thereafter, single clones were screened by PCR amplification for detection of intragenic deletion and sequenced, using the following primers:
SASH3 forward primer: CTCTGACTGTTCAACCCAAGAG
SASH3 reverse primer: GAAATCCTCAAACCCAACCAAAG.
A clone harboring a homozygous 602nt intragenic deletion was isolated and expanded. Lack of SASH3 protein expression was confirmed by western blotting as previously indicated. previously.

Generation of lentiviral vectors and transduction of Jurkat cells and T cell blasts
The *SASH3* cDNA was cloned into the pLVX-EF1alpha-IRES-mcherry Vector (TAKARA Bio USA, CA, USA). Lenti-X 293T cells (TAKARA Bio USA) were plated into T75 flask at a density of 9.4×10^6 cells overnight. The cells were transfected using Lipofectamine 3000 (Invitrogen) following the manufacturer's protocol with either 10μg of the pLVX-EF-1alpha SASH3-IRES-mCherry vector or 10 μg of the pLVX-EF-1α IRES-mCherry vector, and 10 μg of psPAX2 (Addgene) and 1 μg of pMD2.G (Addgene) helper plasmids. At 48h after transfection, viruses were collected from the supernatants and concentrated by 100-fold using Leni-X™ Concentrator (TAKARA Bio USA).
For rescue experiments, control- and P2-derived PBMCs were stimulated with anti-CD3 (eBioscience), anti-CD28 (eBioscience), and 100IU/ml soluble IL-2 (NIH) in RPMI containing 10% FBS. At 48h and 96h after stimulation, 2.5×10^5 cells of the stimulated PBMCs were infected with 10 μl of the concentrated virus in RPMI containing 10% FBS and 10 μg/ml of polybrene by spinning down the cells at 32˚C for 90 minutes. For reconstitution of SASH3

expression in *SASH3*$^{-/-}$ Jurkat cells, 1.0×10^5 cells were infected with 10 µl of the concentrated virus using the same method as for primary T cells.

Analysis of cell proliferation in wild-type, SASH3-deficient and lentivirus-transduced Jurkat cells

An equal number ($2x10^5$) of wild-type, *SASH3*$^{-/-}$ and lentivirus-transduced Jurkat cells was plated in triplicate in 200 µL of RPMI complete medium in a 96-well plate and cultured at 37ºC 5% CO_2. Every 24 hours and up to 4 days of culture, the number of cells contained in each well was counted. Statistical analysis was performed using 2-way ANOVA with multiple comparisons.

Rescue experiments of PLCγ1 phosphorylation with SASH3-expressing lentiviral vector

Control- and P2-derived T cell blasts transduced either with mock or *SASH3* lentiviral vector were serum and IL-2 starved for 1 hours. Cells were stimulated with Dynabeads™ Human T-Activator CD3/CD28 (Invitrogen) for 20 minutes. Total cell lysates were prepared in lysis buffer (50mM Tris pH 7.4, 150mM NaCl, 2mM EDTA, 0.5% Triton X-100 and 0.5% NP40 and halt protease and phosphatase inhibitor cocktail [Sigma]). Samples were adjusted to have equal concentration of total protein, separated by a NuPAGE® Novex® 4-12% Bis-Tris Protein Gels (Life Technology) and transferred to nitrocellulose membranes using the Trans-Blot Turbo Transfer system according to the manufacturer's instruction (Bio-Rad). The membranes were incubated with indicated antibodies, followed by a secondary antibody labeled with HRP (Jackson Immuno Research). The western blot images were acquired and analyzed with C-Digit scanner using Image Studio Software (Li-Cor).

Data sharing

WES data for patients P1, P2, and P3 are part of a larger submission to the database of Genotypes and Phenotypes (dbGaP): https://www.ncbi.nlm.nih.gov/projects/gap/cgi-bin/study.cgi?study_id=phs001899.v1.p1. The dbGaP accession number is phs001899v1.p1, with de-identified dbGaP codes for individual exome data corresponding to 143386-0224060584 (P1), 199316-0305018719 (P2), and 217566-1194544672 (P3).

*P1 is in the first data release, and P2 and P3 are in the current pending second release.

For patient P4, WES have been deposited in BioProject, and can be accessed at: https://dataview.ncbi.nlm.nih.gov/object/PRJNA656252?reviewer=tks8dti8klpq5cgu3vqhpdtjqa. *TRA* repertoire data have been deposited in the Adaptive Biotechnologies website (URL: https://clients.adaptivebiotech.com; username: delmonte-review@adaptivebiotech.com; password: delmonte2020review).

References

1. Richards S, Aziz N, Bale S, et al. Standards and guidelines for the interpretation of sequence variants: a joint consensus recommendation of the American College of Medical Genetics and Genomics and the Association for Molecular Pathology. *Genet Med*. 2015;17(5):405-424.
2. den Dunnen JT, Dalgleish R, Maglott DR, et al. HGVS Recommendations for the Description of Sequence Variants: 2016 Update. *Hum Mutat*. 2016;37(6):564-569.
3. Dobbs K, Tabellini G, Calzoni E, et al. Natural Killer Cells from Patients with Recombinase-Activating Gene and Non-Homologous End Joining Gene Defects Comprise a Higher Frequency of CD56(bright) NKG2A(+++) Cells, and Yet Display Increased Degranulation and Higher Perforin Content. *Front Immunol*. 2017;8:798.
4. Stadinski BD, Shekhar K, Gomez-Tourino I, et al. Hydrophobic CDR3 residues promote the development of self-reactive T cells. *Nat Immunol*. 2016;17(8):946-955.
5. Bosticardo M, Pala F, Calzoni E, et al. Artificial thymic organoids represent a reliable tool to study T-cell differentiation in patients with severe T-cell lymphopenia. *Blood Adv*. 2020;4(12):2611-2616.

Legends to Supplementary Figures

Supplementary Figure1

Flow-cytometry analysis of CD8$^+$ T$_{EMRA}$ cells and CD4$^+$ T helper cells subsets. (A) Expression of the inhibitory receptor PD-1, and death receptor CD95, on CD8$^+$CCR7$^-$CD45RA$^+$ T cells from patients (colored lines) and a healthy control (gray area). (B) Flow cytometry staining of Th subsets from a healthy control and patients P1-P4 upon gating on CD4$^+$CD25^{lo}CD45RA$^-$CXCR5$^-$ cells. Th subsets were defined as follows: Th1, CXCR3$^+$CCR6$^-$; Th17, CXCR3$^-$CCR6$^+$; Th1*, CXCR3$^+$CCR6$^+$.

Supplementary Figure 2

Bone marrow (BM) biopsy studies. (A) Bone marrow core biopsy from P1, showing cellular marrow with reduced M:E ratio. Magnification: 200x. (B) Immunohistochemistry for CD3 expression, showing markedly increased interstitial T cell infiltrate in the bone marrow from P1. Magnification: 200x. (C) Immunohistochemistry showing that the majority of T cells in the bone marrow of P1 are positive for CD8. Magnification: 200x. (D) Flow cytometric analysis of the marrow aspirate from P1 and P2, showing an inverted ration of CD4$^+$ and CD8$^+$ cells in P1. Flow cytometry plots showing that over 50% of the CD8$^+$T cells in the marrow of both P1 and P2 are positive for CD57, consistent with a cytotoxic phenotype in both patients.

Supplementary Figure 3

Flow cytometry analysis of bone marrow B cells. (A) Flow cytometric analysis of B cell subsets in the bone marrow aspirate of P1, P2 and a healthy control. Plots show expression of markers that define various stages of B-cell differentiation. For the first two plots on the left, gating was on LIVE/DEAD$^-$CD45$^+$. For analysis of pro-B cells (third plot from the left), CD22 staining was done on LIVE/DEAD$^-$CD45$^+$CD34$^+$ CD19$^-$ cells. Staining for CD10 and CD20 expression was obtained upon gating on LIVE/DEAD$^-$CD45$^+$CD34$^-$ CD19$^+$ cells to show multiple differentiation stages (small and large preBII, immature, mature B cells), as indicated in the Figure. Expression of CD38 and CD138 was analyzed upon gating on CD34$^+$ CD19$^+$CD20$^-$ CD10$^-$ to show CD38^{hi} CD138$^-$ plasmablasts (PB) and CD138^{hi} and CD38^{hi} plasma cells (PC).

(B) The bar graph shows cumulative frequency of cells at various stages of B cell development in P1 and P2 versus 3 healthy controls.

Supplementary Figure 4

NK cell phenotype and function. (A) Top left row: FACS plot showing NK cell gate ($CD56^+CD20^-CD14^-CD3^-$) in peripheral blood cells from a healthy control and patients P1-P3. Second left row: FACS plot of NK cell subsets according to CD56 and CD16 expression upon gating on total NK cells, in P1 and P2 and in a representative healthy control (CTRL). Third left row and Rows 1, 2, and 3 on the right: FACS plots showing expression of CD57, KIR, NKG2A, and CXCR1 on NK cells in a healthy control and in patients P1 and P2. Patients P3 was not tested for the expression of these markers (n.d. = not done).

(B) Expression of IFN-γ by NK cells from a healthy control (CTRL) and patient P2, with or without stimulation with IL-12 and IL-18. Intracellular IFN-γ production was evaluated by flow-cytometry upon gating on $CD3^-$ $CD56^+$ cells.

(C) NK-cell degranulation, measured as the proportion of $CD3^-$ $CD14^-$ CD20- $CD56^+$ cells expressing CD107a, upon co-culture of PBMCs from P2 and a healthy control (CTRL) with K562 target cells at an effector:target ratio of 1:3 in the presence or absence of IL-2 (100 IU/mL

Supplementary Figure 5

Plasma levels of soluble biomarkers. Levels of soluble biomarkers in patients P1, P2, P3, and in 114 healthy control subjects.

Supplementary Figure 6

SASH3 protein structural model and predicted effects of *SASH3* variants identified in patients**.** (A) 3D model of SASH3 protein from the beginning of the SH3 domain, through the C-terminus, with annotation of domains, phosphorylation sites, and linear motifs for kinase binding. The p.R347C variant occurs within kinase binding site motifs in the C-terminus of SASH3. The truncating p.R288* (B) and p.R245* (C) variants delete part of the SAM domain, as well as the C-terminal region that contains multiple kinase binding motifs. Thus, in addition to the truncating variants removing the SAM domain and thereby impeding dimerization, all three patient variants may alter the post-translational modifications of the protein.

Supplementary Figure 7

Vα7.2 expression by peripheral blood T cells. (A) Representative FACS plot from a healthy control (CTRL) and P2, showing the frequency of Vα-7.2 and MAIT (Vα-7.2$^+$ CD161$^+$) cells upon gating on CD3$^+$ cells. (B) Cumulative frequency of Vα-7.2-expressing T lymphocytes and MAIT cells among CD3$^+$ T cells in healthy controls (n=24 for Vα7.2$^+$ T cells; n= 17 for MAIT cells) and *SASH3*-mutated patients (P1-4).

Supplementary Figure 8

Cell-surface CXCR4 expression in SASH3 deficient T cells. Blood from controls (CTRL) and patients P1 and P2 were stained for cell-surface expression of CD3, CD4, CD8, and CXCR4. The live and single events were selected to analyze for CXCR4 expression on CD4$^+$ T cells (left panels) and CD8$^+$ T cells (right panels) in the SSC-A^{low} (lymphocyte gate) and CD3$^+$ gate. The depicted histograms were obtained by analyzing blood from 2 controls (red) and P1 and P2 patients (blue). Cell-surface CXCR4 was quantified by obtaining ratios of geometric mean fluorescence intensities (MFI) of CXCR4 on indicated T-cell subsets from the controls and the patients.

Supplementary Figure 9

Generation of *SASH3*$^{-/-}$ Jurkat cells. (A) Chromatogram of the DNA sequence of the *SASH3*$^{-/-}$ Jurkat clone carrying a homozygous 602nt deletion (top) and corresponding mapping on the wild-type *SASH3* genomic sequence (bottom). The sequences complementary to the two guide RNAs used to target exon1 and intron 1 are indicated in red. (B) Western blot demonstrating lack of SASH3 protein expression in *SASH3*$^{-/-}$ Jurkat cells. (C) Illustration of the reduced proliferative activity of *SASH3*$^{-/-}$ Jurkat cells as compared to the parental cell line. Statistical significance was assessed by 2-way ANOVA.

Supplementary figures

Figure S1

A

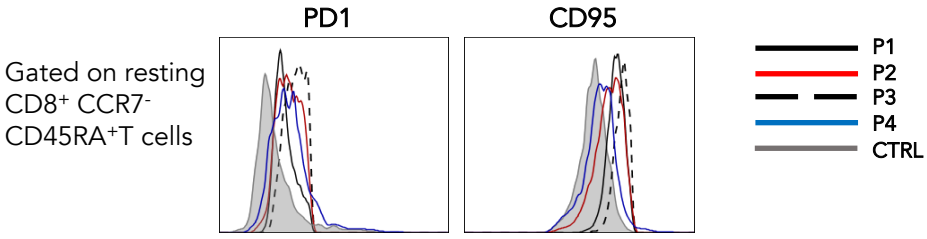
PD1
CD95
Gated on resting
CD8+ CCR7-
CD45RA+T cells
P1
P2
P3
P4
CTRL

B

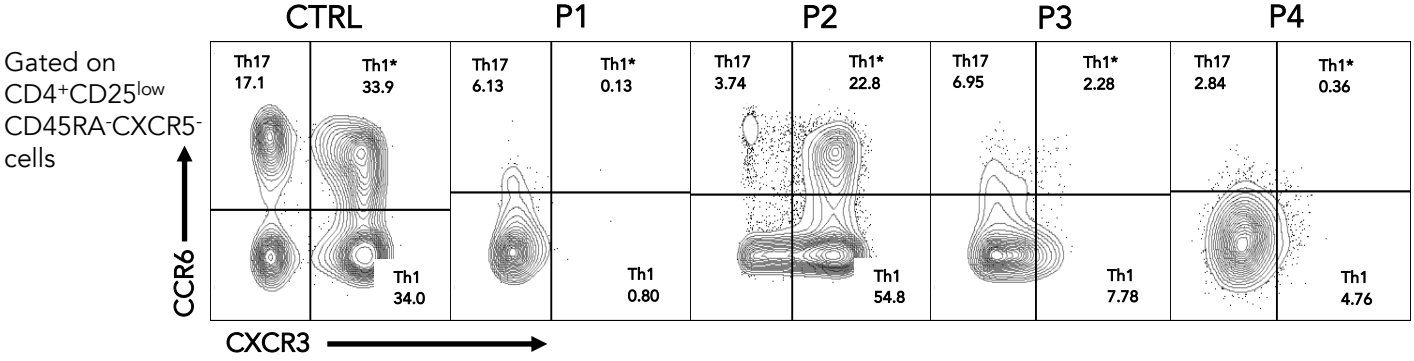
CTRL
P1
P2
P3
P4
Gated on
CD4+CD25low
CD45RA-CXCR5-
cells
Th17 17.1
Th1* 33.9
Th1 34.0
Th17 6.13
Th1* 0.13
Th1 0.80
Th17 3.74
Th1* 22.8
Th1 54.8
Th17 6.95
Th1* 2.28
Th1 7.78
Th17 2.84
Th1* 0.36
Th1 4.76
CCR6
CXCR3

Figure S2

A

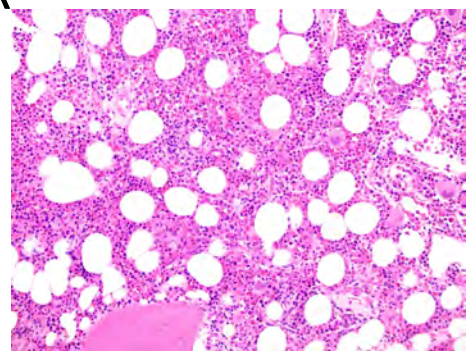

B

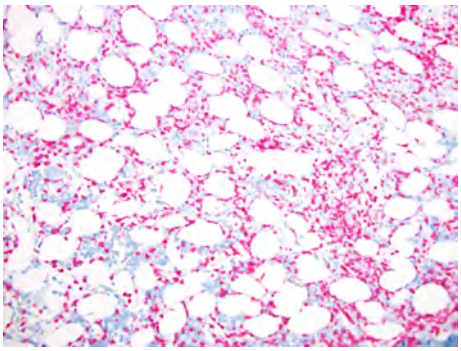

C

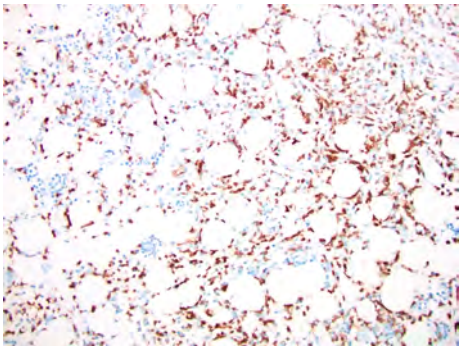

D

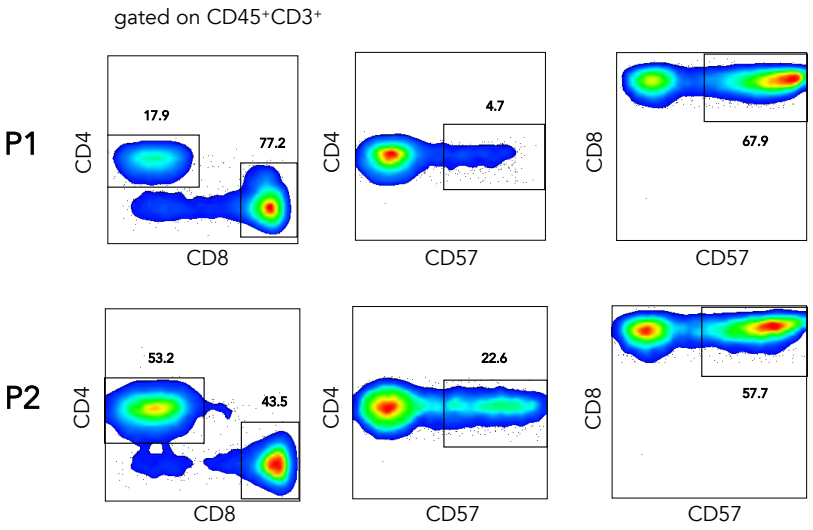

Figure S3

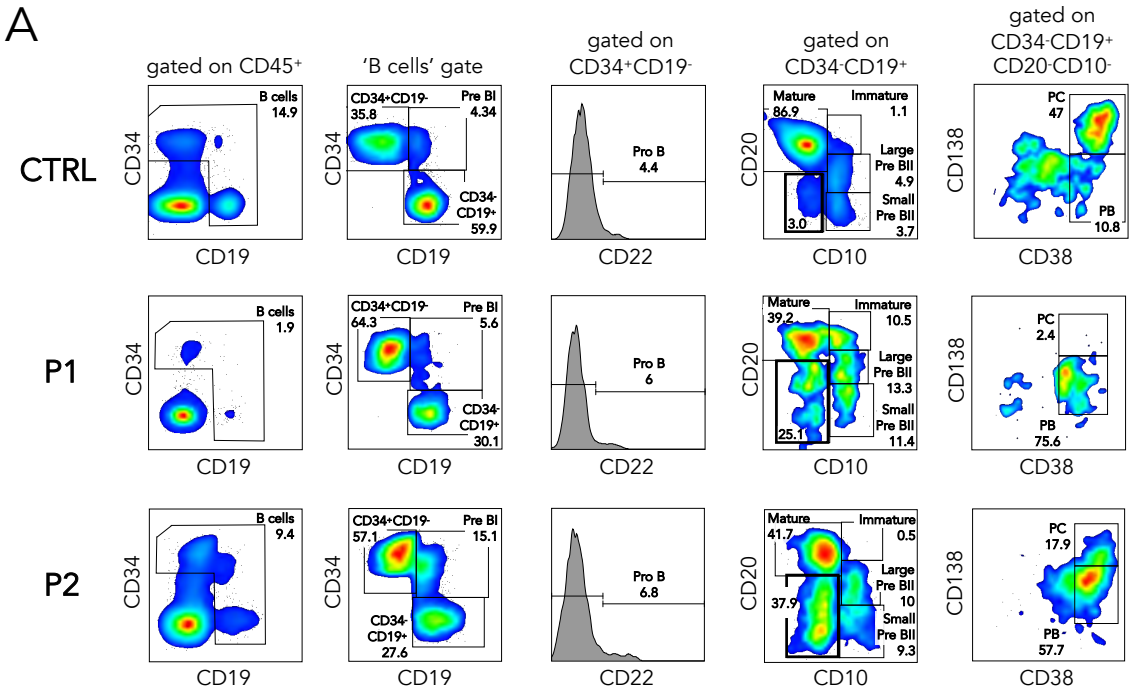
A
gated on CD45+
'B cells' gate
gated on CD34+CD19-
gated on CD34-CD19+
gated on CD34-CD19+ CD20-CD10-
CTRL
P1
P2
CD34
CD19
CD22
CD20
CD10
CD138
CD38
B cells 14.9
CD34+CD19- 35.8
Pre BI 4.34
CD34- CD19+ 59.9
Pro B 4.4
Mature 86.9
Immature 1.1
Large Pre BII 4.9
Small Pre BII 3.7
3.0
PC 47
PB 10.8
B cells 1.9
CD34+CD19- 64.3
Pre BI 5.6
CD34- CD19+ 30.1
Pro B 6
Mature 39.2
Immature 10.5
Large Pre BII 13.3
Small Pre BII 11.4
25.1
PC 2.4
PB 75.6
B cells 9.4
CD34+CD19- 57.1
Pre BI 15.1
CD34- CD19+ 27.6
Pro B 6.8
Mature 41.7
Immature 0.5
Large Pre BII 10
Small Pre BII 9.3
37.9
PC 17.9
PB 57.7

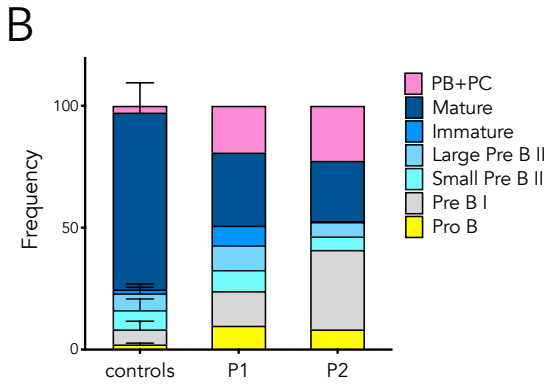
B
Frequency
100
50
0
controls
P1
P2
PB+PC
Mature
Immature
Large Pre B II
Small Pre B II
Pre B I
Pro B

Figure S4

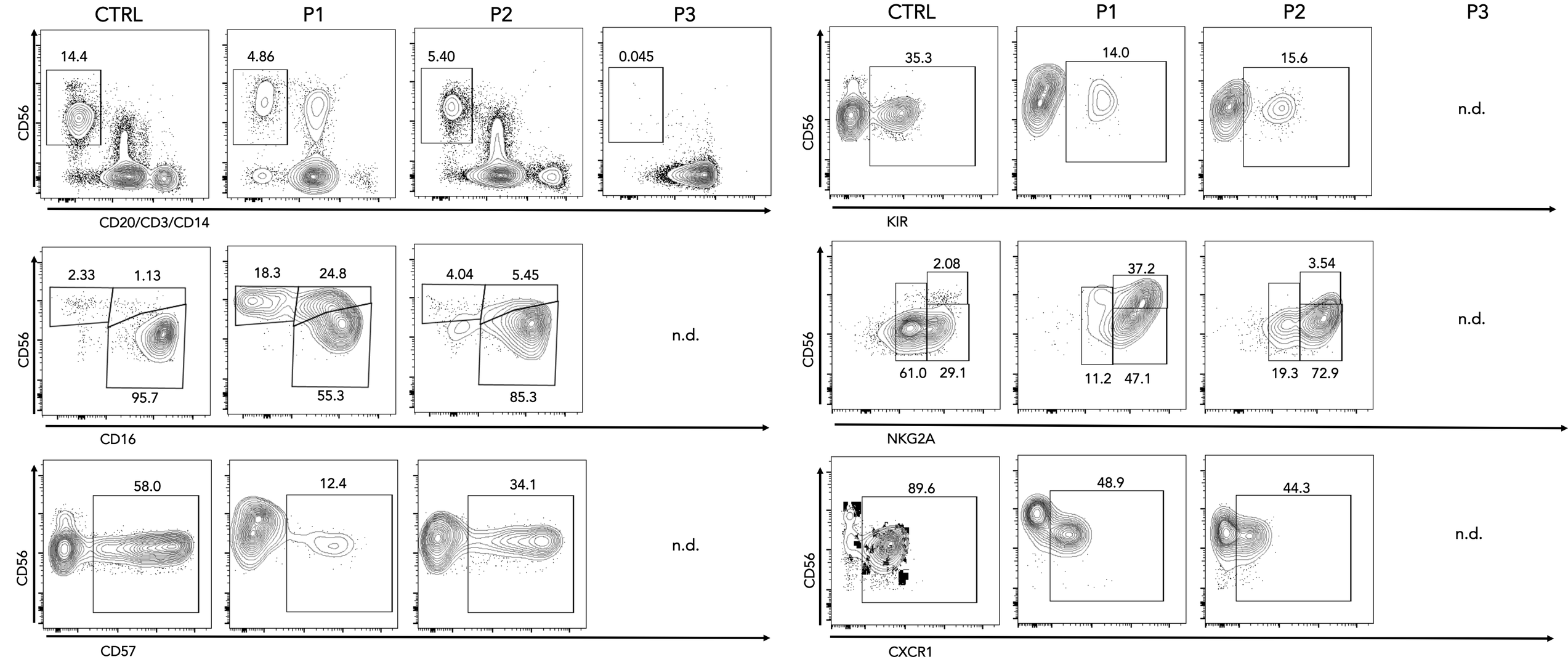
A
CTRL
P1
P2
P3
14.4
4.86
5.40
0.045
CD56
CD20/CD3/CD14
35.3
14.0
15.6
n.d.
KIR
2.33
1.13
95.7
18.3
24.8
55.3
4.04
5.45
85.3
n.d.
CD16
2.08
61.0
29.1
37.2
11.2
47.1
3.54
19.3
72.9
n.d.
NKG2A
58.0
12.4
34.1
n.d.
CD57
89.6
48.9
44.3
n.d.
CXCR1
B
- IL-12/IL-18
+ IL-12/IL-18
CTRL
P2
1.97
66.5
6.54
35.5
CD56
IFN-γ
C
- IL-2
+ IL-2
CTRL
P2
28.7
76.7
42.9
69.1
CD56
CD107a

Figure S5

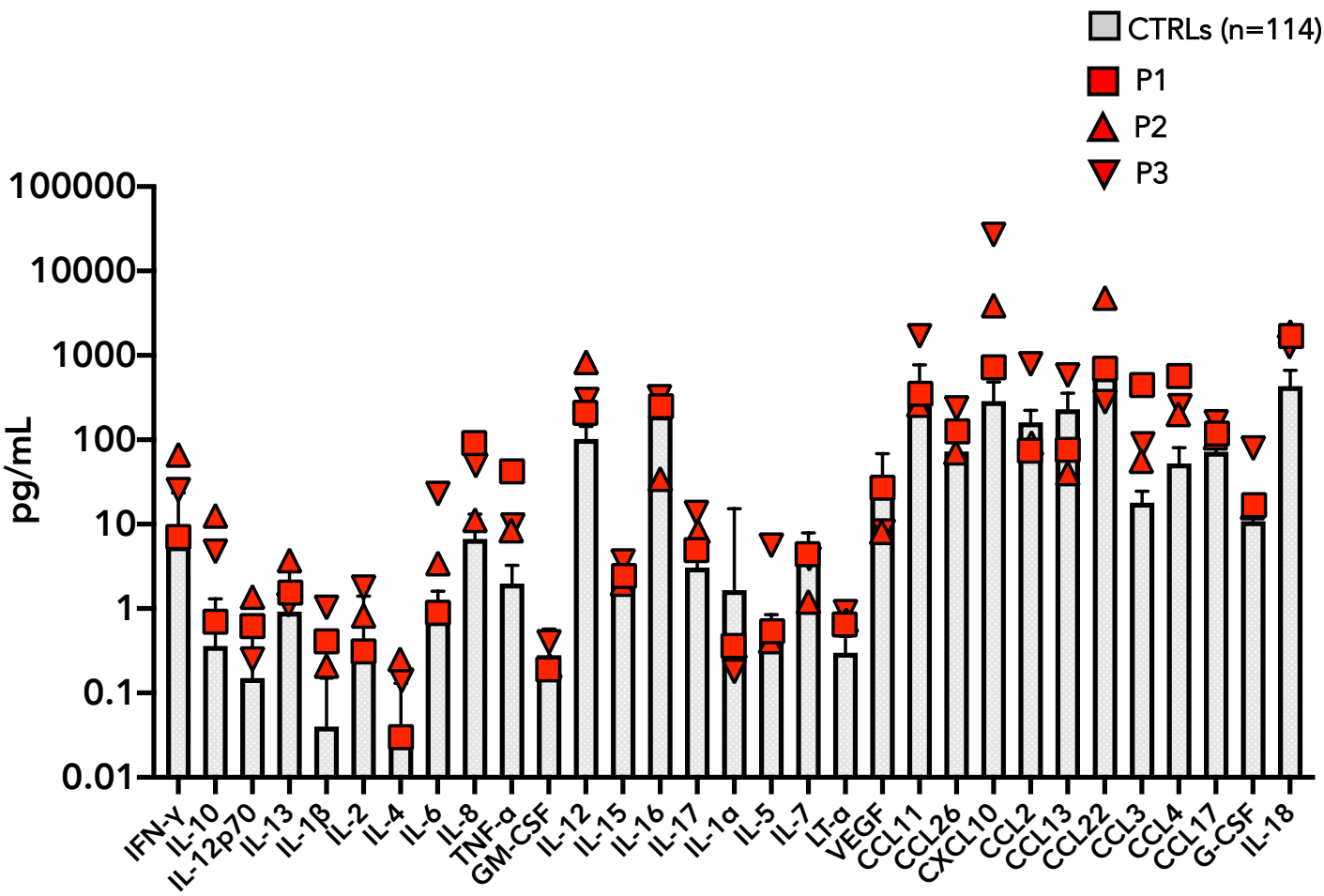
CTRLs (n=114)
P1
P2
P3
100000
10000
1000
100
10
1
0.1
0.01
pg/mL
IFN-γ
IL-10
IL-12p70
IL-13
IL-1β
IL-2
IL-4
IL-6
IL-8
TNF-α
GM-CSF
IL-12
IL-15
IL-16
IL-17
IL-1α
IL-5
IL-7
LT-α
VEGF
CCL11
CCL26
CXCL10
CCL2
CCL13
CCL22
CCL3
CCL4
CCL17
G-CSF
IL-18

Figure S6

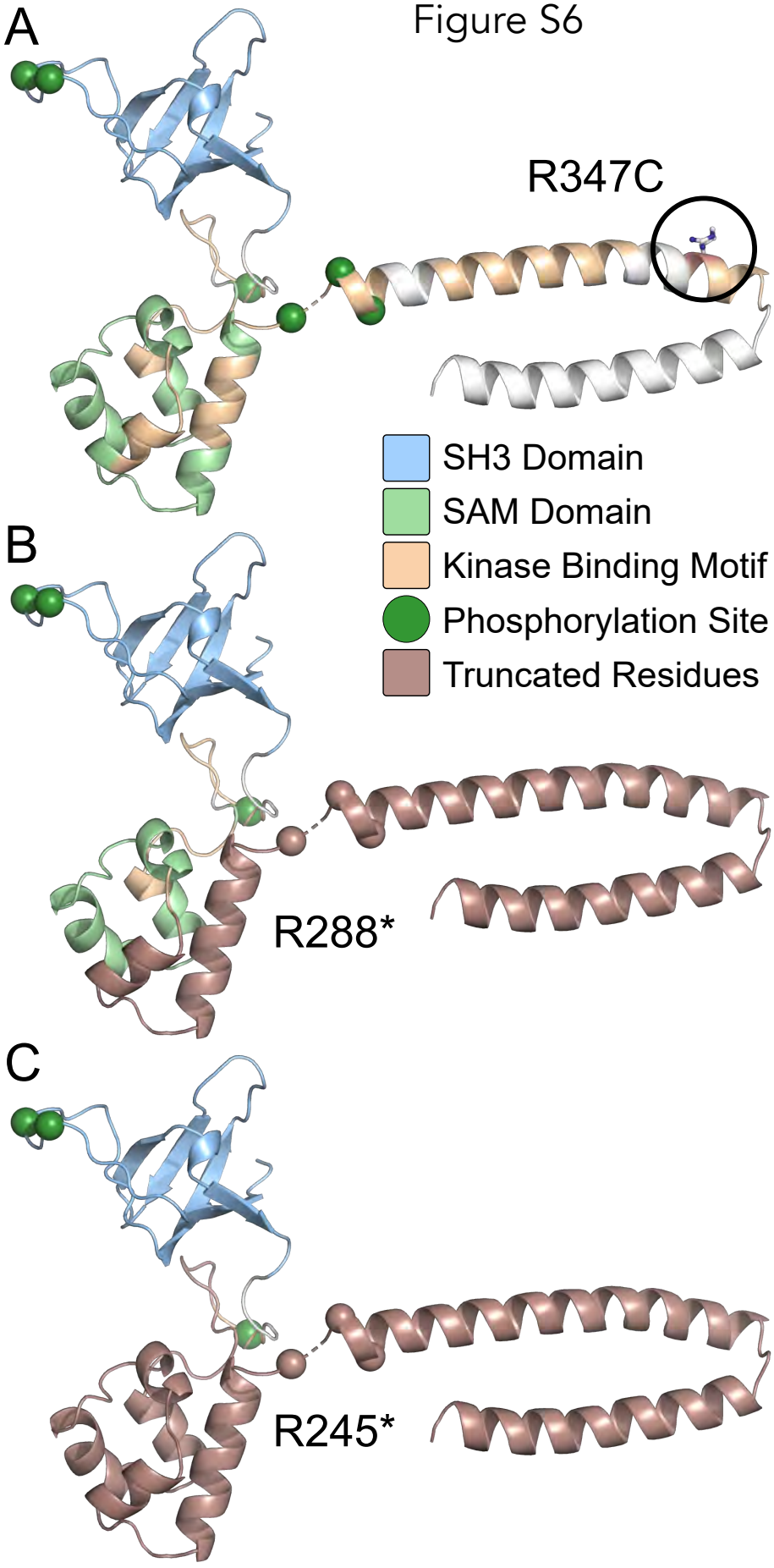
A
R347C
SH3 Domain
SAM Domain
Kinase Binding Motif
Phosphorylation Site
Truncated Residues
B
R288*
C
R245*

Figure S7

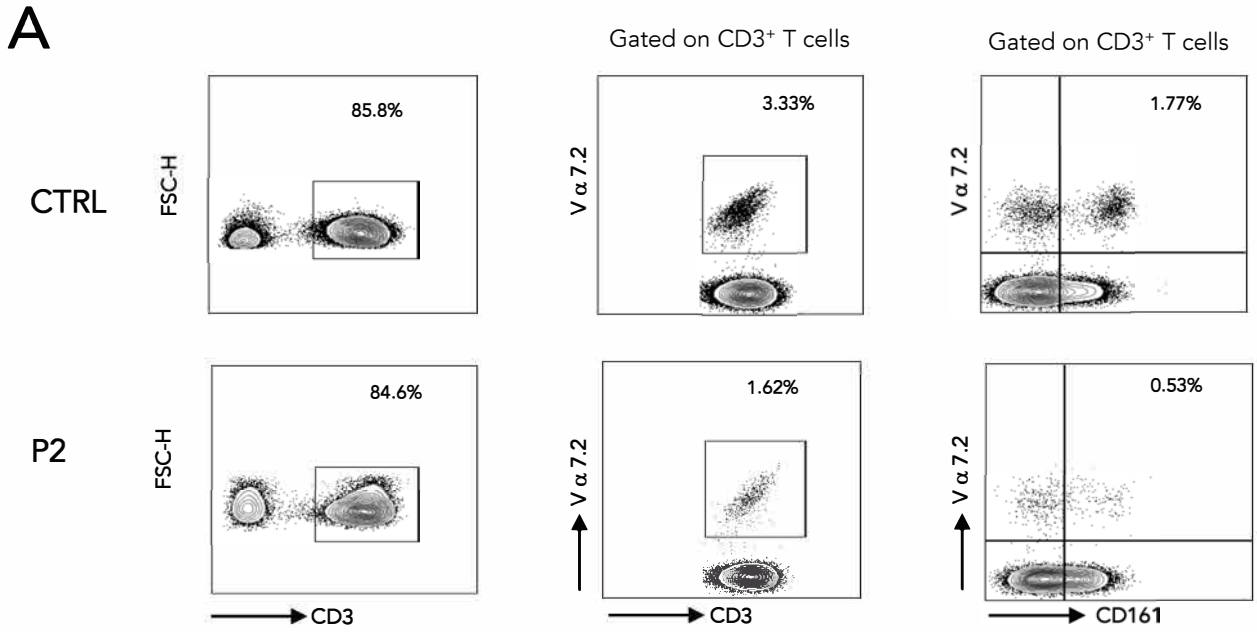
A
Gated on CD3+ T cells
Gated on CD3+ T cells
CTRL
P2
FSC-H
85.8%
3.33%
1.77%
84.6%
1.62%
0.53%
V α 7.2
CD3
CD161

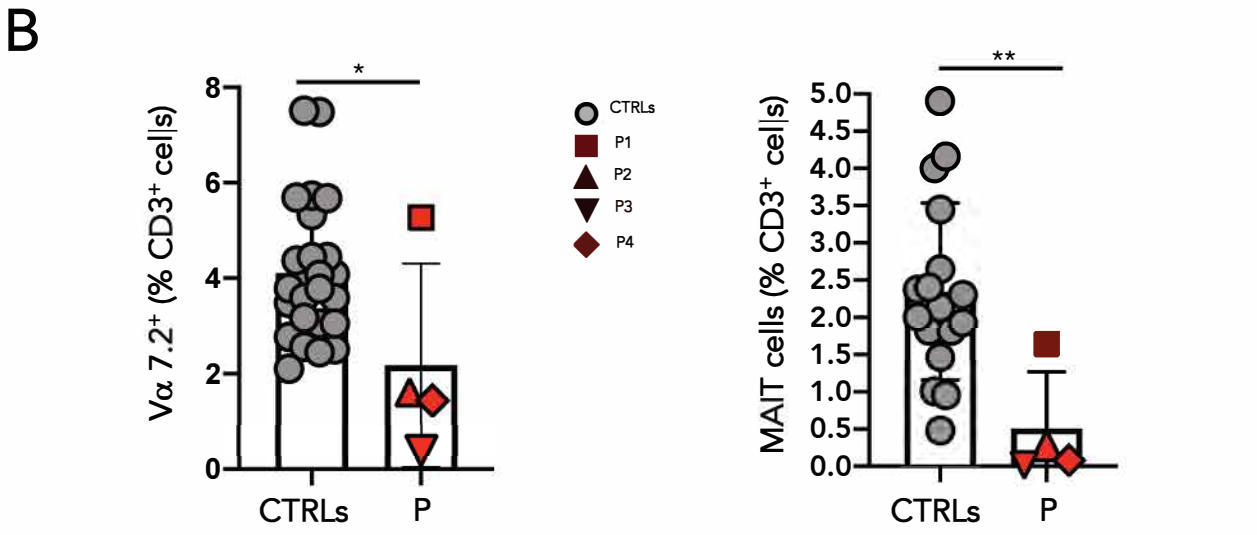
B
Vα 7.2+ (% CD3+ cells)
MAIT cells (% CD3+ cells)
CTRLs
P
P1
P2
P3
P4
*
**

Figure S8

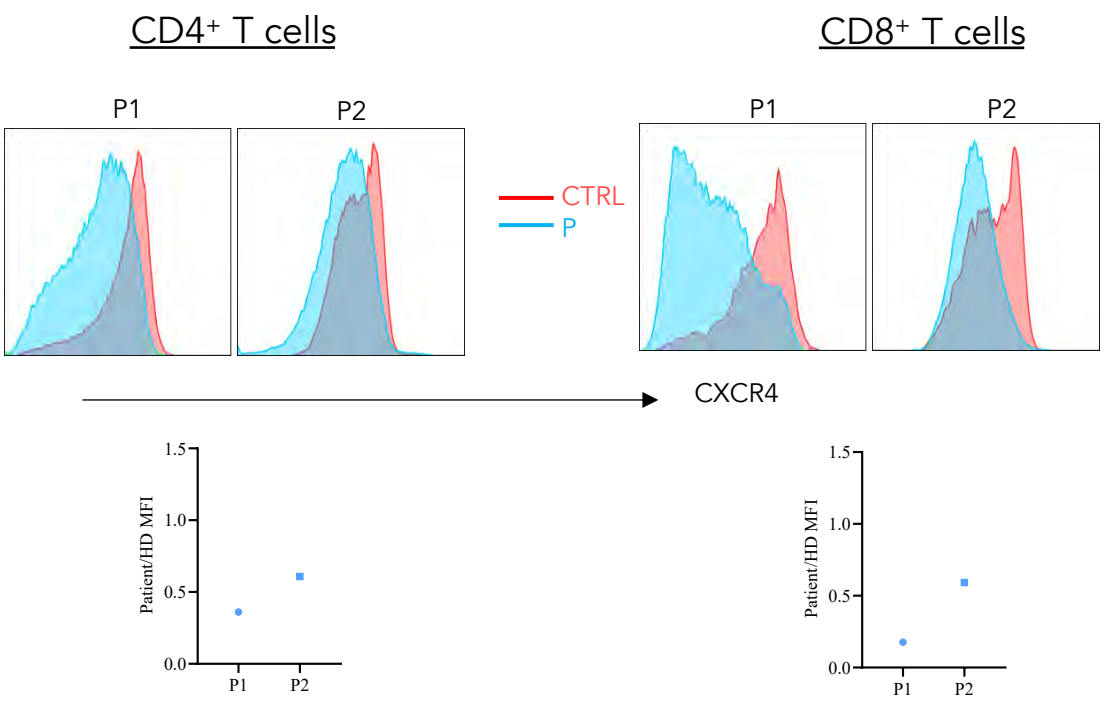
CD4+ T cells
CD8+ T cells
P1
P2
P1
P2
CTRL
P
CXCR4
Patient/HD MFI
1.5
1.0
0.5
0.0
P1
P2
Patient/HD MFI
1.5
1.0
0.5
0.0
P1
P2

Figure S9

A

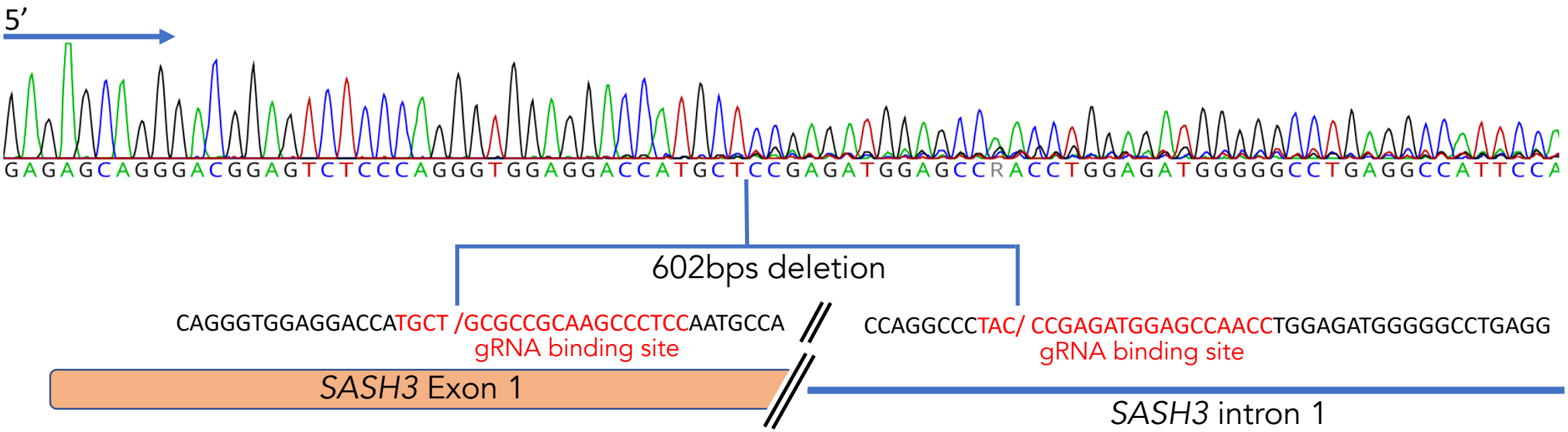

B

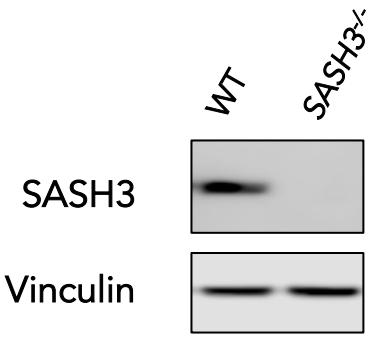

C